NASA/TM—20210020569

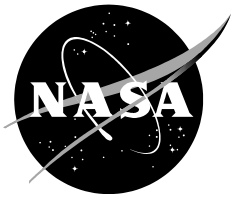

# TESS Data Release Notes:
## Sector 38, DR55

*Michael M. Fausnaugh, Christopher J. Burke*
*Kavli Institute for Astrophysics and Space Science, Massachusetts Institute of Technology, Cambridge, Massachusetts*

*Douglas A. Caldwell*
*SETI Institute, Mountain View, California*

*Jon M. Jenkins*
*NASA Ames Research Center, Moffett Field, California*

*Jeffrey C. Smith, Joseph D. Twicken*
*SETI Institute, Mountain View, California*

*Roland Vanderspek*
*Kavli Institute for Astrophysics and Space Science, Massachusetts Institute of Technology, Cambridge, Massachusetts*

*John P. Doty*
*Noqsi Aerospace Ltd, Billerica, Massachusetts*

*Eric B. Ting*
*NASA Ames Research Center, Moffett Field, California*

*Joel S. Villasenor*
*Kavli Institute for Astrophysics and Space Science, Massachusetts Institute of Technology, Cambridge, Massachusetts*

**August 4, 2021**

NASA STI Program ... in Profile

Since its founding, NASA has been dedicated to the advancement of aeronautics and space science. The NASA scientific and technical information (STI) program plays a key part in helping NASA maintain this important role.
The NASA STI program operates under the auspices of the Agency Chief Information Officer. It collects, organizes, provides for archiving, and disseminates NASA's STI. The NASA STI program provides access to the NTRS Registered and its public interface, the NASA Technical Reports Server, thus providing one of the largest collections of aeronautical and space science STI in the world. Results are published in both non-NASA channels and by NASA in the NASA STI Report Series, which includes the following report types:

- TECHNICAL PUBLICATION. Reports of completed research or a major significant phase of research that present the results of NASA Programs and include extensive data or theoretical analysis. Includes compilations of significant scientific and technical data and information deemed to be of continuing reference value. NASA counterpart of peer-reviewed formal professional papers but has less stringent limitations on manuscript length and extent of graphic presentations.
- TECHNICAL MEMORANDUM.
  Scientific and technical findings that are preliminary or of specialized interest, e.g., quick release reports, working papers, and bibliographies that contain minimal annotation. Does not contain extensive analysis.
- CONTRACTOR REPORT. Scientific and technical findings by NASA-sponsored contractors and grantees.
- CONFERENCE PUBLICATION.
  Collected papers from scientific and technical conferences, symposia, seminars, or other meetings sponsored or co-sponsored by NASA.
- SPECIAL PUBLICATION.
  Scientific, technical, or historical information from NASA programs, projects, and missions, often concerned with subjects having substantial public interest.
- TECHNICAL TRANSLATION.
  English-language translations of foreign scientific and technical material pertinent to NASA's mission.

Specialized services also include organizing and publishing research results, distributing specialized research announcements and feeds, providing information desk and personal search support, and enabling data exchange services.

For more information about the NASA STI program, see the following:

- Access the NASA STI program home page at http://www.sti.nasa.gov
- E-mail your question to help@sti.nasa.gov
- Phone the NASA STI Information Desk at 757-864-9658
- Write to:
  NASA STI Information Desk
  Mail Stop 148
  NASA Langley Research Center
  Hampton, VA 23681-2199

NASA/TM—20210020569

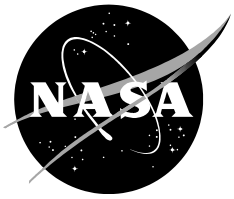

# TESS Data Release Notes:
## Sector 38, DR55

*Michael M. Fausnaugh, Christopher J. Burke*
*Kavli Institute for Astrophysics and Space Science, Massachusetts Institute of Technology, Cambridge, Massachusetts*

*Douglas A. Caldwell*
*SETI Institute, Mountain View, California*

*Jon M. Jenkins*
*NASA Ames Research Center, Moffett Field, California*

*Jeffrey C. Smith, Joseph D. Twicken*
*SETI Institute, Mountain View, California*

*Roland Vanderspek*
*Kavli Institute for Astrophysics and Space Science, Massachusetts Institute of Technology, Cambridge, Massachusetts*

*John P. Doty*
*Noqsi Aerospace Ltd, Billerica, Massachusetts*

*Eric B. Ting*
*NASA Ames Research Center, Moffett Field, California*

*Joel S. Villasenor*
*Kavli Institute for Astrophysics and Space Science, Massachusetts Institute of Technology, Cambridge, Massachusetts*

**August 4, 2021**

## Acknowledgements

These Data Release Notes provide information on the processing and export of data from the Transiting Exoplanet Survey Satellite (TESS). The data products included in this data release are full frame images (FFIs), target pixel files, light curve files, collateral pixel files, cotrending basis vectors (CBVs), and Data Validation (DV) reports, time series, and associated xml files.

These data products were generated by the TESS Science Processing Operations Center (SPOC, Jenkins et al., 2016) at NASA Ames Research Center from data collected by the TESS instrument, which is managed by the TESS Payload Operations Center (POC) at Massachusetts Institute of Technology (MIT). The format and content of these data products are documented in the Science Data Products Description Document (SDPDD)[1]. The SPOC science algorithms are based heavily on those of the Kepler Mission science pipeline, and are described in the Kepler Data Processing Handbook (Jenkins, 2020).[2] The Data Validation algorithms are documented in Twicken et al. (2018) and Li et al. (2019). The TESS Instrument Handbook (Vanderspek et al., 2018) contains more information about the TESS instrument design, detector layout, data properties, and mission operations.

The TESS Mission is funded by NASA's Science Mission Directorate.

This report is available in electronic form at
https://archive.stsci.edu/tess/

[1] https://archive.stsci.edu/missions/tess/doc/EXP-TESS-ARC-ICD-TM-0014-Rev-F.pdf
[2] https://archive.stsci.edu/kepler/manuals/KSCI-19081-003-KDPH.pdf

# 1 Observations

TESS Sector 38 observations include physical orbits 83 and 84 of the spacecraft around the Earth. Data collection was paused for 0.96 days between the orbits to download data. In total, there are 25.74 days of science data collected in Sector 38.

Table 1: Sector 38 Observation times

| | UTC | TJD[a] | Cadence # |
|---|---|---|---|
| Orbit 83 start | 2021-04-29 08:21:04 | 2333.84945 | 796604 |
| Orbit 83 end | 2021-05-11 19:57:04 | 2346.33278 | 805592 |
| Orbit 84 start | 2021-05-12 19:01:04 | 2347.29389 | 806284 |
| Orbit 84 end | 2021-05-26 01:11:03 | 2360.55083 | 815829 |

[a] TJD = TESS JD = JD - 2,457,000.0

The spacecraft was pointing at RA (J2000): 195.7176°; Dec (J2000): −67.8307°; Roll: 139.3519°. See the TESS project Sector 38 observation page[3] for the coordinates of the spacecraft pointing and center field-of-view of each camera. Fields-of-view for each camera can be found at the TESS Guest Investigator Office observations status page.[4] The detailed target list for both 2-minute and 20-second data, as well as the Guest Investigator target lists, can be found at the Sector 38 observation page and the observations status page.

## 1.1 Update to the TIC

The TESS Input Catalog (TIC) was updated to v8.2 for data processing in Sector 38. The TIC v8.2 update identifies newly discovered `ARTIFACT` and `DUPLICATE` sources that were not flagged in the v8.0/8.1 revisions of the TIC. TIC stars labeled `ARTIFACT` are not stars, but rather non-astrophysical objects caused by diffraction spikes, image ghosting, bleed trails, or other similar phenomena. A TIC star labeled `DUPLICATE` is effectively an exact copy of of another TIC star: the other TIC star is called the "parent" and is considered the 'official' entry for that star. The detailed description of these labels can be found in the MAST archives.

The Sector 38 targets were selected using TIC v8.1 and processed with TIC v8.2. As a result, several dozen targets identified in TIC v8.2 as `DUPLICATE` or `ARTIFACT` were processed. For newly flagged `ARTIFACT` sources, target pixel files are produced, but no light curves or DV products are produced. For `DUPLICATE` sources, if the "parent" TIC ID was not also a target, target pixel files, light curves, and DV products are produced using the `DUPLICATE` TIC ID in the file name. If the "parent" was also observed, the full set of target pixel files, light curves, and DV products are produced for the parent, but only target pixel files are produced for the `DUPLICATE`. These target pixel files do not include a background correction.

In total, there were 9 `ARTIFACT` and 56 `DUPLICATE` sources selected in Sector 38 with no light curves or DV products. A table of the TIC IDs without light curves, their flags, and

[3] https://tess.mit.edu/observations/sector-38

[4] https://heasarc.gsfc.nasa.gov/docs/tess/status.html

parent star TIC IDs (for which light curves exist) is given in Appendix A as well as in a supplemental file[5].

### 1.2 Notes on Individual Targets

For the 20-second cadence data, one bright star (471011144) with a large pixel stamp was not processed in the photometric pipeline. For the 2-minute cadence data, 13 bright stars (Tmag $\lesssim$ 1.8) with large pixel stamps were not processed in the photometric pipeline. Target pixel files with original and calibrated pixel data are provided, but no light curves were produced. Note that the TPF files do not include a background correction for stars without light curves. Furthermore, cosmic rays are not identified in pixel data for 20-second target stars without light curves. The affected TIC IDs of the 2-minute data are 272314138, 255559489, 399646462, 471011144, 471011145, 38877693, 128116539, 440960978, 179323446, 262834160, 314113726, 328329822, 290794924.

Six target stars (404768847, 300015238, 261862960, 177635952, 261862960, 300015238) are blended with comparably bright stars—the contaminating flux for these objects is very large, and the resulting photometry for such targets is expected to be unreliable.

Three stars (255560740, 272482277, 450568600) are close enough to the bleed trail from a brighter star that the photometry is likely unreliable.

Two targets (336343562, 440953551) have disjoint apertures in order to avoid bleed trails from brighter stars and likely have unreliable photometry.

### 1.3 Spacecraft Pointing and Momentum dumps

Camera 4 alone was used for guiding in orbit 83 of Sector 38. Both Cameras 1 and 4 were used for guiding in orbit 84. A single momentum dump was performed halfway through each orbit. Figure 1 summarizes the pointing performance over the course of the sector based on Fine Pointing telemetry.

### 1.4 Scattered Light

Figure 2 shows the median value of the background estimate for all targets on a given CCD as a function of time. Figure 3 shows the angle between each camera's boresight and the Earth or Moon—this figure can be used to identify periods affected by scattered light and the relative contributions of the Earth and Moon to the image backgrounds.

In Sector 38, there is scattered light for most of both orbits.

## 2 Data Anomaly Flags

See the SDPDD (§9) for a list of data quality flags and the associated binary values used for TESS data, and the TESS Instrument Handbook for a more detailed description of each flag.

[5] https://archive.stsci.edu/missions/tess/catalogs/targetinfo/tess_sector_38_drn55_artdupnolc_v01.txt

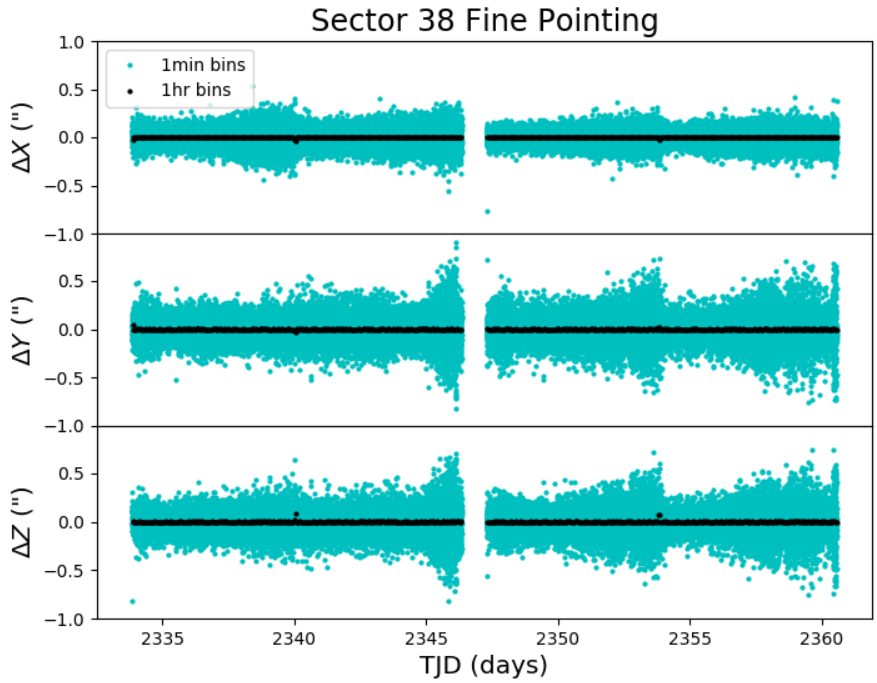


Figure 1: The delta-quaternions from each camera have been converted to spacecraft frame, binned to 1 minute and 1 hour, and averaged across cameras. Long-term trends (such as those caused by differential velocity aberration) have also been removed. The ΔX/ΔY directions represent offsets along the the detectors' rows/columns, while the ΔZ direction represents spacecraft roll.

The following flags were not used in Sector 38: bits 1, 2, and 9 (Attitude Tweak, Safe Mode, and Discontinuity).

Cadences marked with bits 3, 4, 6, and 12 (Coarse Point, Earth Point, Reaction Wheel Desaturation Event, and Straylight) were marked based on spacecraft telemetry.

Cadences marked with bit 5 and 10 (Argabrightening Events and Impulsive Outlier) were identified by the SPOC pipeline. Bit 5 marks a sudden change in the background measurements. In practice, bit 5 flags are caused by rapidly changing glints and unstable pointing at times near momentum dumps. Bit 10 marks an outlier identified by PDC and omitted from the cotrending procedure.

The 20-second data mode includes cadences marked with bit 7 and 11 (Cosmic Ray in Optimal Aperture and Cosmic Ray in Collateral Pixel). These flags indicate cadences affected by cosmic rays that are removed by the pipeline, and can be found in both the TPF and LC files. The data provided in the archive products are corrected for cosmic rays, and a `FITS` table extension in the TPF and Collateral Pixel File details the cosmic rays identified and removed by the pipeline at the pixel level.

Cadences marked with bit 8 (Manual Exclude) are ignored by PDC, TPS, and DV for cotrending and transit searches. In Sector 38, these cadences were identified using spacecraft telemetry from the fine pointing system. All cadences with pointing excursions >7 arcsec (0.3 pixel) were flagged for manual exclude. Figure 4 also shows an assessment of the performance

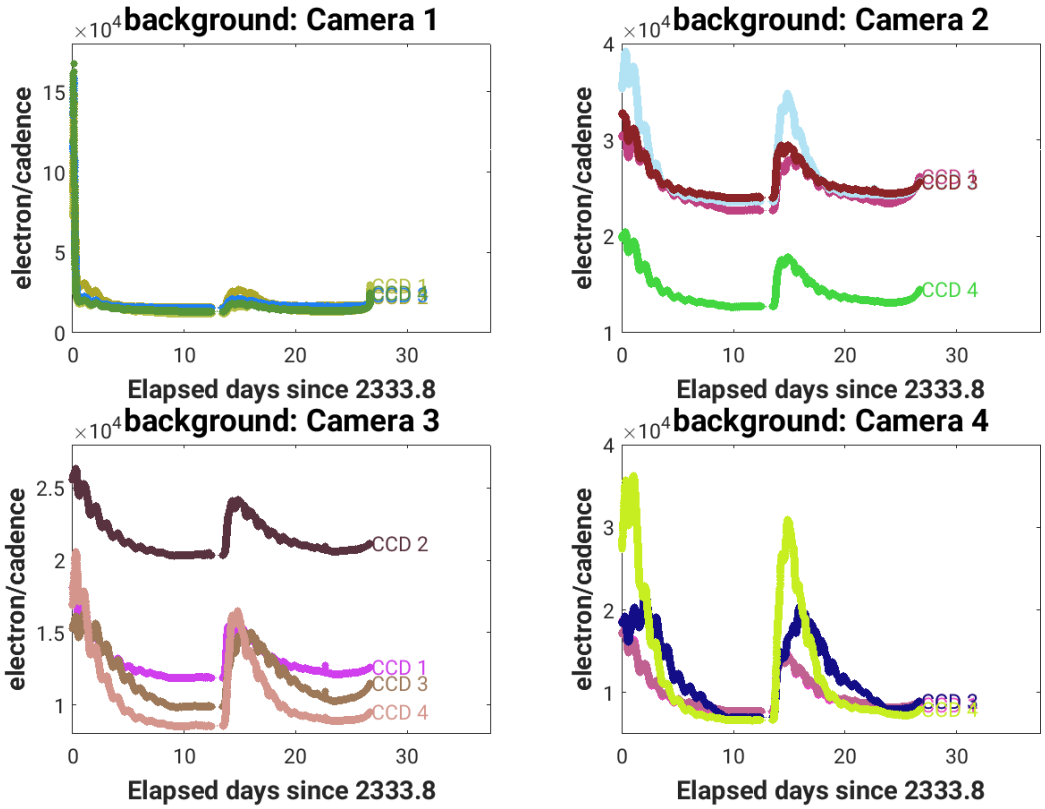


Figure 2: Median background flux across all targets on a given CCD in each camera. The changes are caused by variations in the orientation and distance of the Earth and Moon.

of the cotrending based on the final set of manual excludes.

The predicted stray light flag (bit 12, value 2048) is marked in the FFIs and flags times when the Earth/Moon are near the camera FOVs and may interfere with guiding or saturate the detectors. We strongly recommend that users inspect the FFI data before removing images marked with bit 12, because this bit is set based on predictions from mission planning and is known to be conservative with respect to the quality of data usable for analysis.

The predicted stray light flag (bit 12) is disabled for the 2-minute and 20-second data products. The scattered light exclude flag (bit 13, value 4096) identifies cadences at which individual targets are affected by scattered light

If the Earth/Moon interference is strong enough to saturate the detector, all targets on a CCD slice will be affected and the data are unusable. Cadences with bad calibrations due to saturation are now explicitly marked with bit 15 (value 16384, "Bad Calibration Exclude"). For some cadences, the majority of targets on a CCD may be flagged for scattered light and not enough valid data remains to derive cotrending basis vectors in PDC. No systematic error correction can be applied at these times. This situation is identified by bit 16 (value 32768, "Insufficient Targets for Error Correction Exclude").

FFIs were only marked with bits 3, 6, 8, 12, and 15 (Coarse Point, Reaction Wheel Desaturation Events, Manual Exclude, Straylight, and Bad Calibration Exclude). Only one FFI is affected by each momentum dump. There are no WCS coordinates for FFIs that

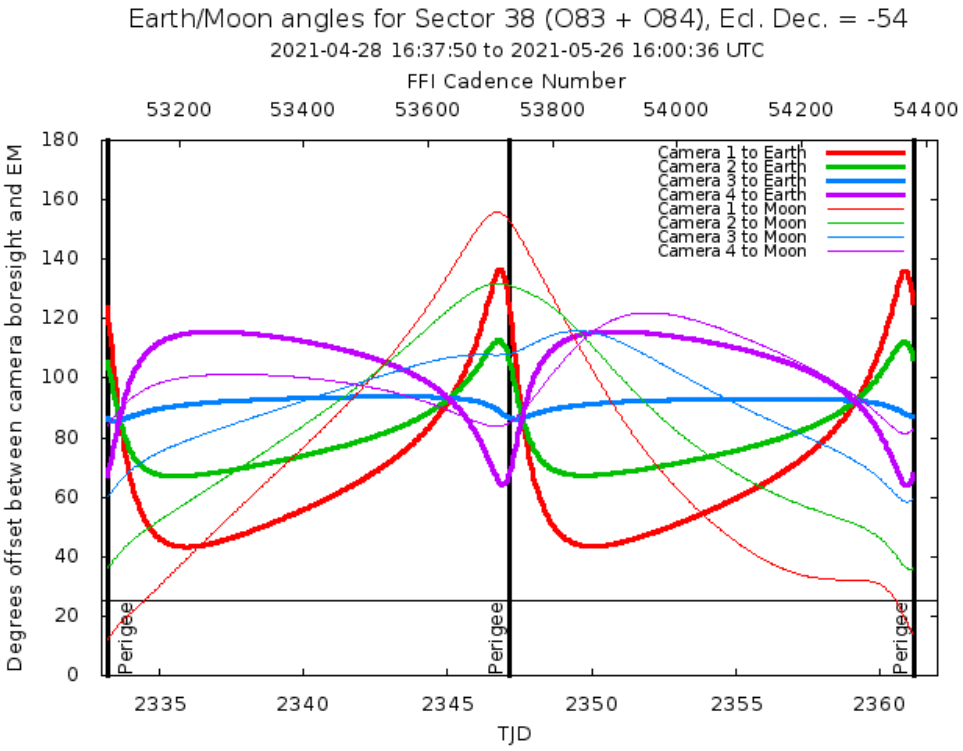


Figure 3: Angle between the four camera boresights and the Earth/Moon as a function of time. When the Earth is within $\sim 25°$ of a camera's boresight, transiting planet searches may be compromised by high levels of scattered light. At larger angles, up to $\sim 35°$, scattered light patterns and complicated structures may be visible. At yet larger angles, low level patchy features may be visible. Scattered light from the Moon is generally only noticeable below $\sim 35°$. This figure can be used to identify periods affected by scattered light and the relative contributions of the Earth and Moon to the background. However, the background intensity and locations of scattered light features depend on additional factors, such as the Earth/Moon azimuth and distance from the spacecraft.

coincide with momentum dumps.

# 3 Anomalous Effects

## 3.1 Smear Correction Issues

The following columns were impacted by bright stars in the science frame, and/or upper buffer rows, and/or lower science frame rows, which bleed into the upper serial register resulting in an overestimated smear correction.

- Camera 1, Ccd 2, Column 245 - Star Alpha Lupi
- Camera 2, Ccd 2, Column 942 - Star Alpha Centauri
- Camera 4, Ccd 1, Column 1862 - Star HD 39475

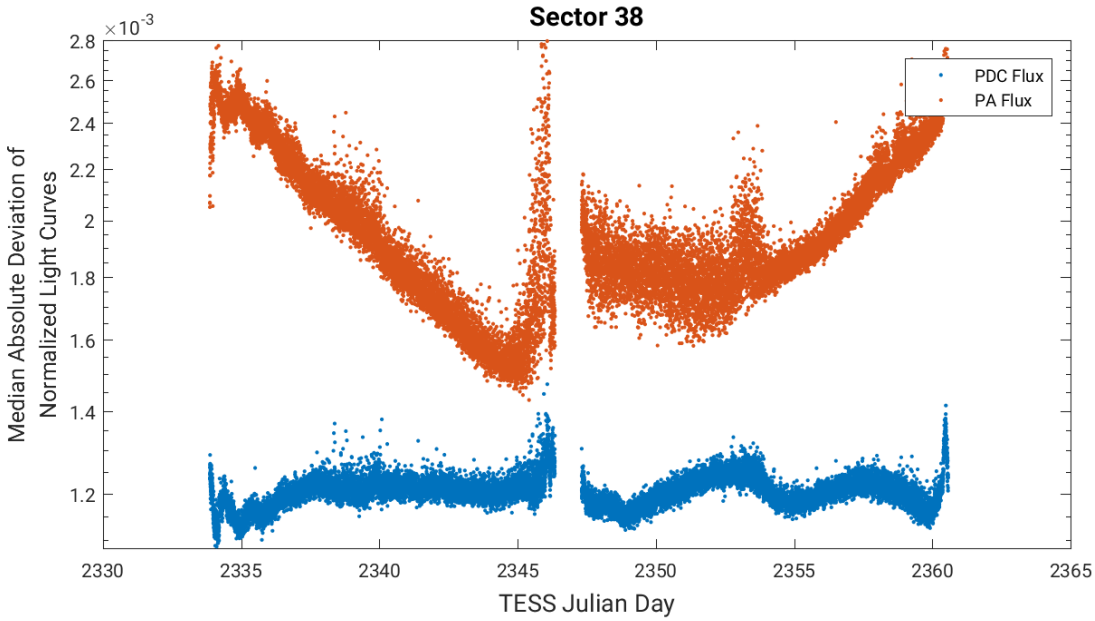


Figure 4: Median absolute deviation (MAD) for the two-minute cadence data from Sector 38, showing the performance of the cotrending after identifying Manual Exclude data quality flags. The MAD is calculated in each cadence across stars with flux variations less than 1% for both the PA (red) and PDC (blue) light curves, where each light curve is normalized by its median flux value. The scatter in the PA light curves is much higher than that for the PDC light curves, and the outliers in the PA light curves are largely absent from the PDC light curves due to the use of the anomaly flags.

- Camera 4, Ccd 2, Column 1180 - Star Alpha Pictoris
- Camera 4, Ccd 3, Column 1012 - Star HD 49076
- Camera 4, Ccd 3, Column 1510 - Star HD 45796
- Camera 4, Ccd 4, Column 157 - Star Epsilon Doradus
- Camera 4, Ccd 4, Column 1996 - Star HD 25938

## 3.2 Fireflies and Fireworks

Table 2 lists all firefly and fireworks events for Sector 38. These phenomena are small, spatially extended, comet-like features in the images—created by sunlit particles in the camera FOV—that may appear one or two at a time (fireflies) or in large groups (fireworks). See the TESS Instrument Handbook for a more complete description.

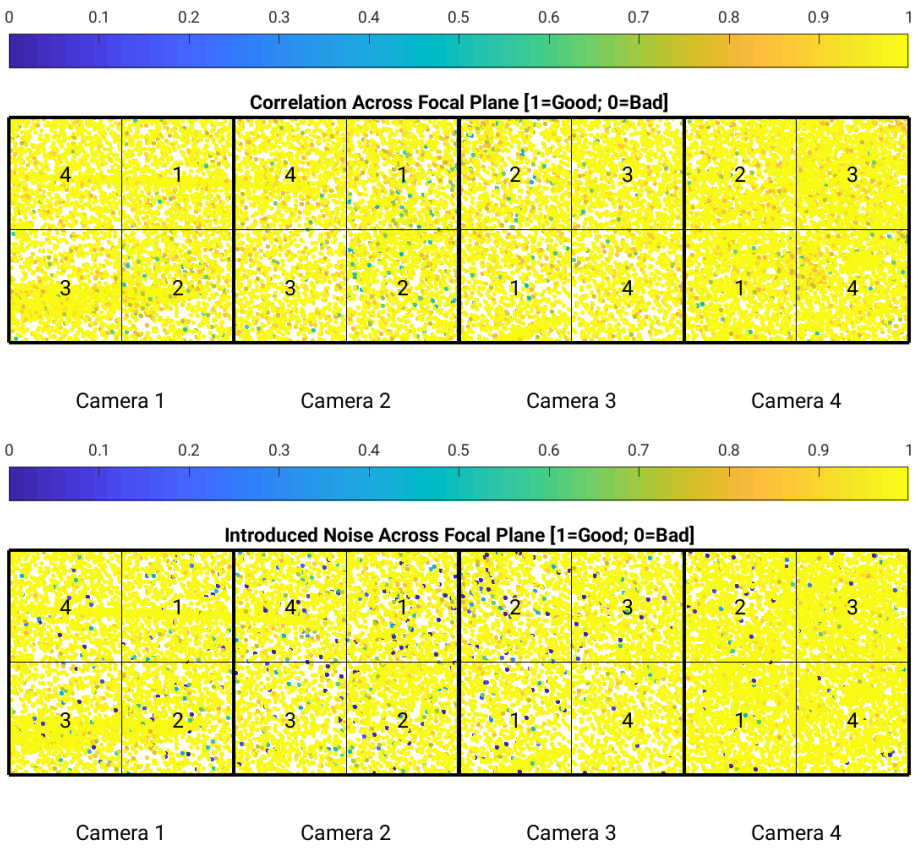


Figure 5: PDC residual correlation goodness metric (top panel) and PDC introduced noise goodness metric (bottom panel) for the two-minute cadence data. The metric values are shown on a focal plane map indicating the camera and CCD location of each target. The correlation goodness metric is calibrated such that a value greater than 0.8 means there is less than 10% mean absolute correlation between the target under study and all other targets on the CCD. The introduced noise metric is calibrated such that a value greater than 0.8 means the power in broad-band introduced noise is below the level of uncertainties in the flux values.

# 4 Pipeline Performance and Results

## 4.1 Light Curves and Photometric Precision

Figure 5 gives the PDC goodness metrics for the two-minute cadence data, with residual correlation goodness and introduced noise goodness shown on a scale between 0 (bad) and 1 (good). The performance of PDC is very good and generally uniform over most of the field of view. Figure 6 shows the achieved Combined Differential Photometric Precision (CDPP) at 1-hour timescales for all two-minute targets.

## 4.2 Transit Search and Data Validation

In Sector 38, the two-minute light curves of 19922 targets were subjected to the transit search in TPS. Of these, Threshold Crossing Events (TCEs) at the 7.1 $\sigma$ level were generated for

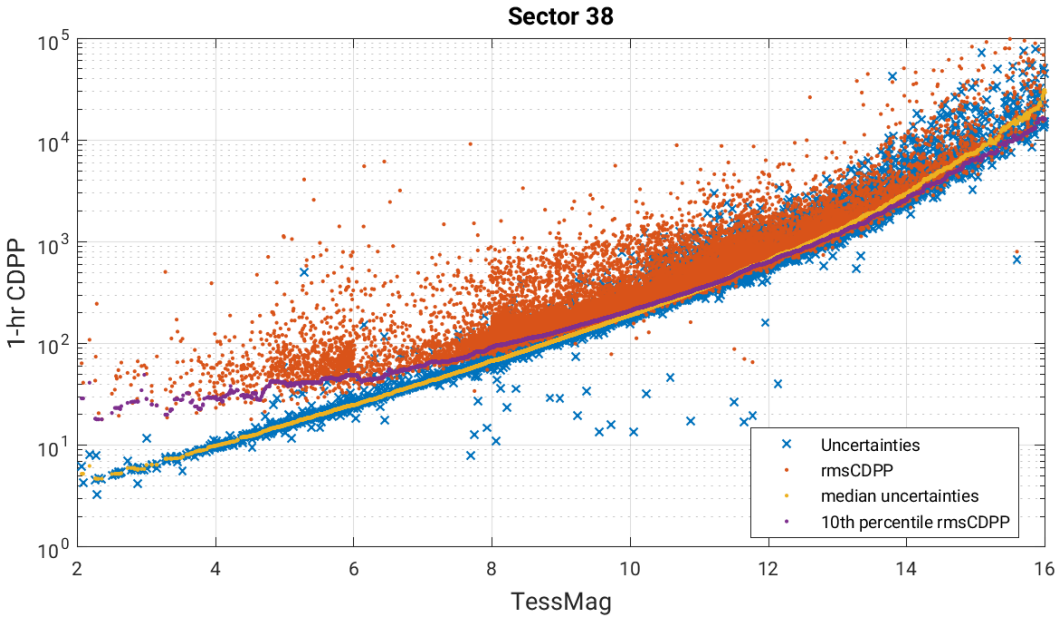


Figure 6: 1-hour CDPP. The red points are the RMS CDPP measurements for the 19922 light curves from Sector 38 plotted as a function of TESS magnitude. The blue x's are the uncertainties, scaled to 1-hour timescale. The purple curve is a moving 10th percentile of the RMS CDPP measurements, and the gold curve is a moving median of the 1-hr uncertainties.

Table 2: Sector Fireflies and Fireworks

| FFI Start | FFI End | Cameras | Description |
|---|---|---|---|
| 2021130125904 | 2021130134904 | 1 | Fireflies |
| 2021132200904 | 2021132201904 | 1 | Firefly |
| 2021133003904 | 2021133005904 | 1,2 | Fireworks |
| 2021139214904 | 2021139215904 | 3 | Firefly |
| 2021141234904 | 2021141235904 | 1,2,3,4 | Fireworks |

1569 targets.

We employed an iterative method when conducting the Sector 38 transit search. The top panel of Figure 7 shows the number of TCEs at a given cadence that exhibit a transit signal from an initial run of TPS. The 3-$\sigma$ peaks were used to define de-emphasis weights for a second run of TPS, the results of which are shown in the bottom panel of Figure 7. The final set of TCEs and the results reported here are based on the second run of TPS. The values of the adopted de-emphasis weights are provided in the DV timeseries data products for targets with TCEs.

The top panel of Figure 8 shows the distribution of orbital periods for the final set of TCEs found in Sector 38. The vertical histogram in the right panel of Figure 8 shows the distribution of transit depths derived from limb-darkened transiting planet model fits for TCEs. The model transit depths range down to the order of 100 ppm, but the bulk of the transit depths are considerably larger.

A search for additional TCEs in potential multiple planet systems was conducted in DV through calls to TPS. A total of 2287 TCEs were ultimately identified in the SPOC pipeline on 1569 unique target stars. Table 3 provides a breakdown of the number of TCEs by target. Note that targets with large numbers of TCEs are likely to include false positives.

Table 3: Sector 38 TCE Numbers

| Number of TCEs | Number of Targets | Total TCEs |
|---|---|---|
| 1 | 1027 | 1027 |
| 2 | 418 | 836 |
| 3 | 88 | 264 |
| 4 | 24 | 96 |
| 5 | 8 | 40 |
| 6 | 4 | 24 |
| – | 1569 | 2287 |

## Appendix A

The following table lists TIC IDs of Sector 38 targets that were flagged as `ARTIFACT` or `DUPLICATE` in v8.2 of the TIC. For all `DUPLICATE` sources, the parent star was observed and data products for the parent should be used. For the tabulated targets, target pixel files (without background subtraction) are available, but light curves and DV products are not available.

Table 4: Sector 38 `ARTIFACT` and `DUPLICATE` Sources Without Light Curves

| TIC ID | Disposition | Parent TIC ID |
|---|---|---|
| 438816209 | ARTIFACT | None |
| 311838201 | ARTIFACT | None |
| 454542043 | ARTIFACT | None |
| 307435285 | ARTIFACT | None |
| 277025286 | ARTIFACT | None |
| 272429505 | ARTIFACT | None |
| 349765573 | ARTIFACT | None |
| 350345734 | ARTIFACT | None |
| 382099937 | ARTIFACT | None |
| 1052669346 | DUPLICATE | 159197295 |
| 1055540348 | DUPLICATE | 365714263 |
| 1174374790 | DUPLICATE | 160059455 |
| 1153701123 | DUPLICATE | 335452175 |
| 1154626342 | DUPLICATE | 307525994 |
| 1172055696 | DUPLICATE | 442615457 |
| 1175170993 | DUPLICATE | 7958125 |

| | | |
|---|---|---|
| 1175735713 | DUPLICATE | 464680263 |
| 1054773682 | DUPLICATE | 107615807 |
| 1055641614 | DUPLICATE | 60868905 |
| 1176007927 | DUPLICATE | 48228593 |
| 1176133308 | DUPLICATE | 46937 |
| 1176537766 | DUPLICATE | 146816 |
| 976942547 | DUPLICATE | 450827144 |
| 1012412298 | DUPLICATE | 342721199 |
| 1121747911 | DUPLICATE | 258708320 |
| 1121965222 | DUPLICATE | 259424304 |
| 1042640024 | DUPLICATE | 446356458 |
| 1045658573 | DUPLICATE | 208791781 |
| 1047826265 | DUPLICATE | 419943828 |
| 1049425449 | DUPLICATE | 329296696 |
| 954686803 | DUPLICATE | 357468855 |
| 955210093 | DUPLICATE | 360946710 |
| 957424540 | DUPLICATE | 335001650 |
| 1003457120 | DUPLICATE | 418616237 |
| 1003843902 | DUPLICATE | 418385999 |
| 1005005237 | DUPLICATE | 396693868 |
| 1104778329 | DUPLICATE | 402726344 |
| 905806736 | DUPLICATE | 399195694 |
| 906129712 | DUPLICATE | 399149882 |
| 906427792 | DUPLICATE | 392244914 |
| 907007356 | DUPLICATE | 295570470 |
| 910280575 | DUPLICATE | 280514622 |
| 911984593 | DUPLICATE | 390760531 |
| 917004504 | DUPLICATE | 305892425 |
| 958526150 | DUPLICATE | 405081305 |
| 976001213 | DUPLICATE | 308633483 |
| 843245247 | DUPLICATE | 452604247 |
| 843283157 | DUPLICATE | 452591868 |
| 844588625 | DUPLICATE | 372313154 |
| 846550604 | DUPLICATE | 362937274 |
| 847861543 | DUPLICATE | 378035923 |
| 724107963 | DUPLICATE | 392013575 |
| 842776931 | DUPLICATE | 388238508 |
| 904264399 | DUPLICATE | 395011859 |
| 765325999 | DUPLICATE | 349376367 |
| 765419969 | DUPLICATE | 167552090 |
| 765444982 | DUPLICATE | 349154302 |
| 765561912 | DUPLICATE | 349683698 |
| 804804891 | DUPLICATE | 272429506 |
| 734548585 | DUPLICATE | 350744311 |
| 737163462 | DUPLICATE | 150357613 |

| | | |
|---|---|---|
| 737165368 | DUPLICATE | 150391195 |
| 650429704 | DUPLICATE | 237923291 |
| 684767046 | DUPLICATE | 55745232 |
| 733027940 | DUPLICATE | 149248196 |

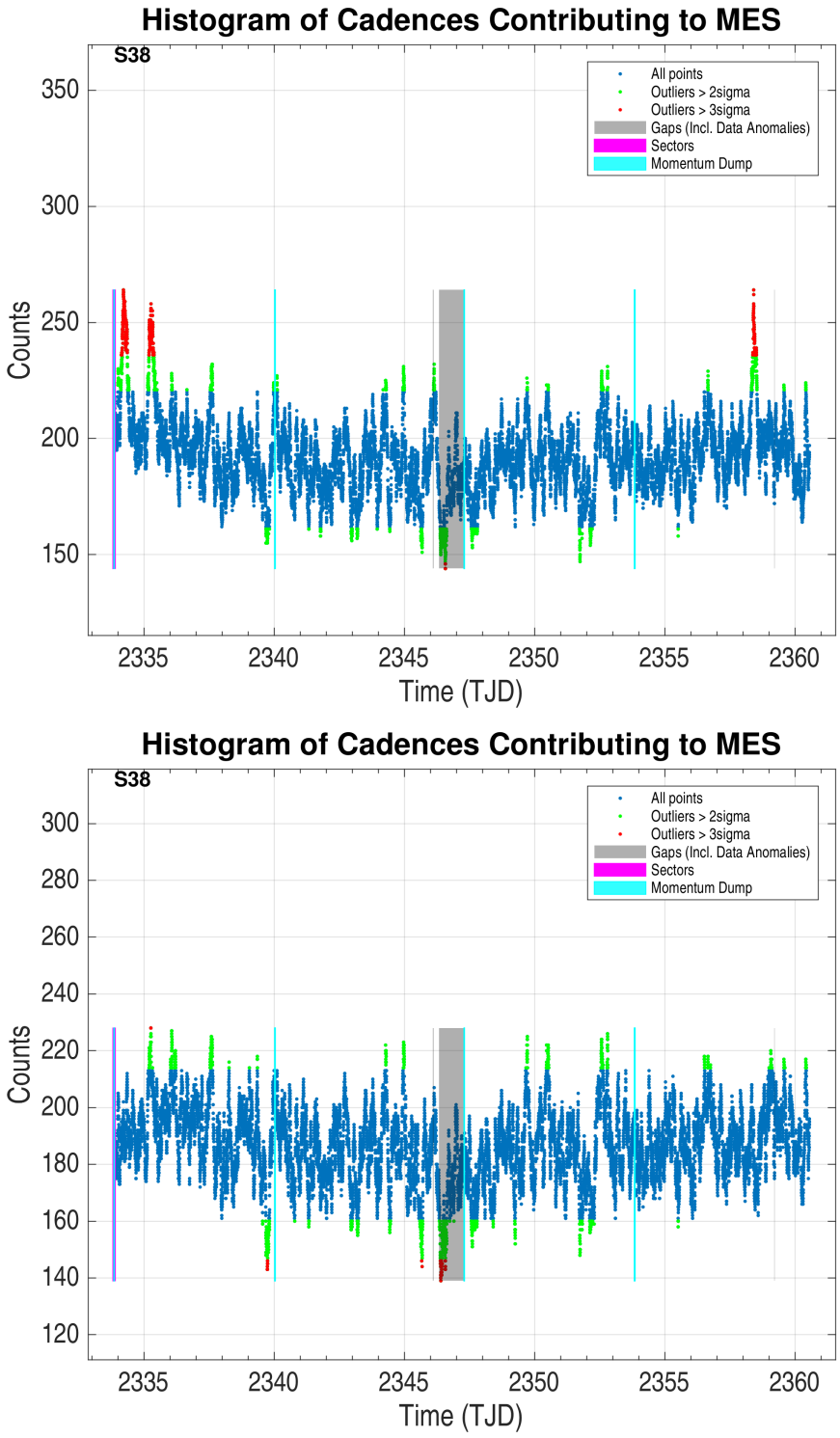


Figure 7: Top panel: Number of TCEs at a given cadence exhibiting a transit signal, based on an initial run of TPS. Any isolated peaks are caused by single events that result in spurious TCEs. These peaks were used to define de-emphasis weights that suppress problematic epochs for the transit detection statistics in a second iteration of TPS. Bottom panel: Results from the second run of TPS.

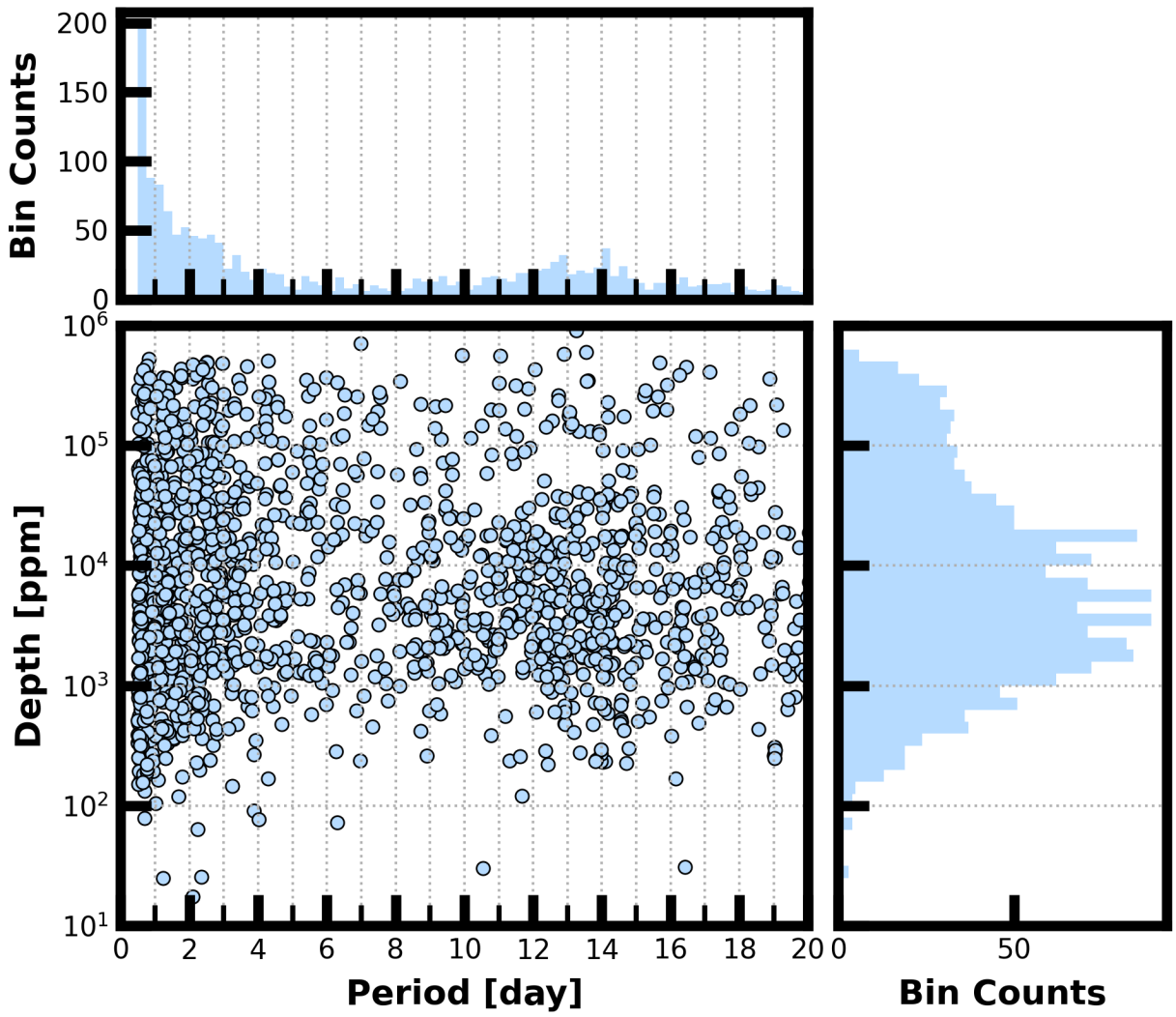


Figure 8: Lower Left Panel: Transit depth as a function of orbital period for the 2287 TCEs identified for the Sector 38 search. For enhanced visibility of long period detections, TCEs with orbital period <0.5 days are not shown. Reported depth comes from the DV limb-darkened transit fit depth when available, and the DV trapezoid model fit depth when not available. Top Panel: Orbital period distribution of the TCEs shown in the lower left panel. Right Panel: Transit depth distribution for the TCEs shown in the lower left panel.

# References


Jenkins, J. M. 2020, Kepler Data Processing Handbook: Overview of the Science Operations Center, Tech. rep., NASA Ames Research Center

Jenkins, J. M., Twicken, J. D., McCauliff, S., et al. 2016, in Proc. SPIE, Vol. 9913, Software and Cyberinfrastructure for Astronomy IV, 99133E, doi: 10.1117/12.2233418

Li, J., Tenenbaum, P., Twicken, J. D., et al. 2019, *PASP*, 131, 024506, doi: 10.1088/1538-3873/aaf44d

Twicken, J. D., Catanzarite, J. H., Clarke, B. D., et al. 2018, *PASP*, 130, 064502, doi: 10.1088/1538-3873/aab694

Vanderspek, R., Doty, J., Fausnaugh, M., et al. 2018, TESS Instrument Handbook, Tech. rep., Kavli Institute for Astrophysics and Space Science, Massachusetts Institute of Technology

# Acronyms and Abbreviation List

**BTJD** Barycentric-corrected TESS Julian Date

**CAL** Calibration Pipeline Module

**CBV** Cotrending Basis Vector

**CCD** Charge Coupled Device

**CDPP** Combined Differential Photometric Precision

**COA** Compute Optimal Aperture Pipeline Module

**CSCI** Computer Software Configuration Item

**CTE** Charge Transfer Efficiency

**Dec** Declination

**DR** Data Release

**DV** Data Validation Pipeline Module

**DVA** Differential Velocity Aberration

**FFI** Full Frame Image

**FIN** FFI Index Number

**FITS** Flexible Image Transport System

**FOV** Field of View

**FPG** Focal Plane Geometry model

**KDPH** Kepler Data Processing Handbook

**KIH** Kepler Instrument Handbook

**KOI** Kepler Object of Interest

**MAD** Median Absolute Deviation

**MAP** Maximum A Posteriori

**MAST** Mikulski Archive for Space Telescopes

**MES** Multiple Event Statistic

**NAS** NASA Advanced Supercomputing Division

**PA** Photometric Analysis Pipeline Module

**PDC** Pre-Search Data Conditioning Pipeline Module

**PDC-MAP** Pre-Search Data Conditioning Maximum A Posteriori algorithm

**PDC-msMAP** Pre-Search Data Conditioning Multiscale Maximum A Posteriori algorithm

**PDF** Portable Document Format

**POC** Payload Operations Center

**POU** Propagation of Uncertainties

**ppm** Parts-per-million

**PRF** Pixel Response Function

**RA** Right Ascension

**RMS** Root Mean Square

**SAP** Simple Aperture Photometry

**SDPDD** Science Data Products Description Document

**SNR** Signal-to-Noise Ratio

**SPOC** Science Processing Operations Center

**SVD** Singular Value Decomposition

**TCE** Threshold Crossing Event

**TESS** Transiting Exoplanet Survey Satellite

**TIC** TESS Input Catalog

**TIH** TESS Instrument Handbook

**TJD** TESS Julian Date

**TOI** TESS Object of Interest

**TPS** Transiting Planet Search Pipeline Module

**UTC** Coordinated Universal Time

**WCS** World Coordinate System

**XML** Extensible Markup Language